Quantum aberrations: Entangling photons with Zernike polynomials

H. Avetisyan [*]
Alikahanyan National Laboratory (Yerevan Physics Institute), 2 Alikhanyan Brothers Street, Yerevan 0036, Armenia

G. Nikoghosyan
Yerevan State University, 1 Alex Manoogian Street, Yerevan 0025, Armenia

(Received 27 May 2025; accepted 23 September 2025; published 15 October 2025)

We introduce Zernike polynomials as a novel degree of freedom for encoding quantum information in the spatial structure of photons. Building on their orthogonality and completeness over the unit disk, we develop a framework for generating, manipulating, and detecting photons in Zernike modes, and propose methods for realizing single-photon and two-photon Zernike wave packets. We demonstrate analytically that two-photon states generated via spontaneous parametric down-conversion exhibit mode entanglement in the Zernike basis, with correlations arising from selection rules enforced by Clebsch-Gordan coefficients. Our results open a new pathway for structured spatial entanglement, complementary to schemes based on Laguerre-Gaussian or Hermite-Gaussian modes, and suggest practical experimental implementations based on holographic modulation and optical Fourier techniques.

DOI: 10.1103/dbfr-f46b

I. INTRODUCTION

Structured spatial modes of light have emerged as a powerful resource for quantum information processing. In particular, encoding quantum states in orbital angular momentum or Hermite-Gaussian spatial modes has led to demonstrations of high-dimensional entanglement, quantum communication protocols, and quantum information processing [1–7]. However, extending the set of spatial mode bases beyond conventional families such as Hermite-Gaussian and Laguerre-Gaussian opens new possibilities for control, robustness, and efficiency.

Historically, a great deal of attention has been paid to the Zernike modes as a complete set of polynomials to expand the aberration phase on the exit pupil of an imaging optical system. We direct the reader to Zernike's groundbreaking 1934 paper [8], Nijboer's 1942 thesis [9] on the diffraction theory of aberrations, and to Born and Wolf [10], particularly Chap. 9, Secs. 9.1 to 9.4, and Appendix VII, for an exploration of the early development of the Nijboer-Zernike theory and a comprehensive review of it, including the mathematical properties of the polynomials. Here we mention only that Zernike disk polynomials $Z(x, y)$ are distinguished from other sets of polynomials by their elegant invariance properties: when the coordinate axes are rotated about the origin, each polynomial is transformed into a polynomial of the same form [11] in the sense that $Z(x, y) = G(\theta)Z(x', y')$ (x', y' are the rotated coordinates). More importantly, each Zernike polynomial represents an optimally balanced combination of Seidel power series terms [9], minimizing variance across the pupil, or equivalently, maximizing the intensity in Gaussian focus [12]. Furthermore, Zernike polynomials are mathematically related to generalized spherical harmonics, which arise in the solution of Laplace's equation in higher-dimensional spaces [13]. It should be noted that the true origin of the ad hoc operator introduced by Zernike has not yet been adequately addressed. A recent study by Abgaryan *et al.* [14] reported that, via an appropriate canonical (gauge) transformation, the Zernike Hamiltonian can be mapped exactly to that of a free particle constrained to a hemispherical surface of a two-dimensional (2D) sphere.

Relatively little work has been carried out in the quantum domain using Zernike modes or the Zernike Hamiltonian [15], leaving significant opportunities for further exploration and development in this area. For example, Zernike modes can be used to represent qudits (d-dimensional quantum states). For example, Zernike modes Z_n^m can be used to represent qudits, with the mode indices n and m serving as quantum numbers. These indices can be manipulated, that is, raised or lowered, using optical masks generated through interferometric techniques [16]. One can also measure the Zernike modes using the same masks to convert the Zernike modes into plane-wave modes. In quantum information schemes, first-order Zernike modes can be manipulated in a manner analogous to the linear and circular polarization of electromagnetic fields [17]. Devices can be constructed to act on these modes in a way analogous to the operation of polarizing beam splitters, half-wave plates, and quarter-wave plates [18,19]. As a result, first-order Zernike modes can form a basis for encoding qubits and enabling single-qubit rotations. We outline methods for constructing photon states and defining field operators in the Zernike basis. Moreover, we show that photon pairs

*Contact author: h.avetisyan@yerphi.am

entangled in Zernike modes can be generated through the process of spontaneous parametric down-conversion (SPDC). Spatial mode entanglement of down-converted photons has already been demonstrated, both theoretically and experimentally, for Laguerre-Gaussian and Hermite-Gaussian modes [20,21].

Although Hermite-Gaussian and Laguerre-Gaussian modes are widely used in quantum optics and are compatible with circularly symmetric systems, they are not specifically tailored to represent optical aberrations. In contrast, Zernike modes form a complete orthogonal basis on the unit disk and directly correspond to common wavefront aberrations, making them naturally suited for describing and manipulating spatial distortions in pupil-limited systems. Zernike modes are ideally suited for quantum protocols involving optical imperfections, adaptive optics, or pupil-limited imaging systems.

In this work, we present the first complete quantum framework for the use of Zernike modes in quantum optics. Our new results include the following:

(i) A formal construction of photon creation and annihilation operators in the Zernike basis;

(ii) Analytical expressions for single-photon and two-photon wave packets in this basis;

(iii) Demonstration of two-photon entanglement via SPDC, with selection rules governed by Clebsch-Gordan coefficients;

(iv) Experimental strategies for preparing, transforming, and detecting Zernike modes; and

(v) Discussion of specific quantum tasks, such as aberration sensing and robust communication, where Zernike entanglement offers distinct advantages.

These results extend the scope of spatial-mode-based quantum optics by introducing a new, physically grounded basis that is especially well matched to practical optical systems exhibiting pupil-limited or aberrated behavior. We note that this study addresses free-space propagation through diffraction-limited optics; random media such as a turbulent atmosphere will be considered in a separate work. While Zernike modes are not paraxial eigenmodes like Laguerre-Gaussian beams, the pupil-to-image mapping in Eq. (18) preserves the expansion coefficients of Eq. (1), enabling exact reconstruction of the field in the image plane of an ideal optical system. This property makes Zernike encoding attractive in aperture-limited contexts.

II. ZERNIKE POLYNOMIALS AND SOME OF THEIR PROPERTIES

Zernike polynomials are not only a convenient mathematical basis; they are rooted in the physics of optical aberrations. In classical optics, they provide a complete and orthogonal basis over the unit disk, allowing for compact representation of wavefront distortions across a circular pupil. Each low-order Zernike polynomial corresponds to a distinct aberration type commonly encountered in imaging systems. For instance, Z_2^0 represents defocus, $Z_3^{\pm1}$ corresponds to coma, and $Z_2^{\pm2}$ describes astigmatism. Higher-order terms represent more complex distortions such as spherical aberration or trefoil. These modes have been extensively used in optical testing, adaptive optics, and phase correction systems,

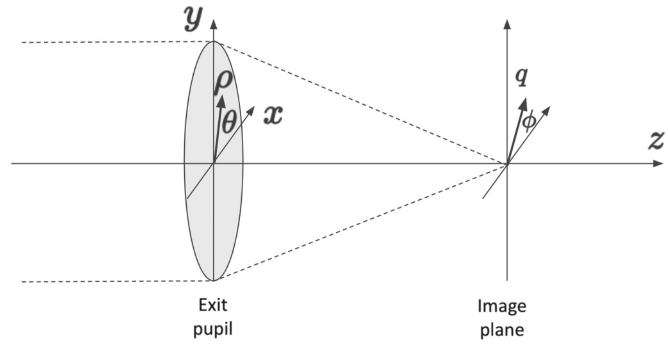

FIG. 1. The basic optical configuration. A wavefront in the exit pupil coming from a point in the object plane (not shown) converges towards the image plane. The position on the exit pupil is defined by the polar coordinates (ρ, θ); the position in the image plane region is defined by the polar coordinate system (q, ϕ).

where the aberration phase $\Phi(\rho, \theta)$ is expanded in the Zernike basis and manipulated directly using deformable mirrors or phase masks. In interferometry, the Zernike coefficients are extracted to quantify system imperfections, while in vision science they are used to characterize human eye aberrations [22,23].

By leveraging this strong physical foundation, we propose (see Sec. IV) extending the use of Zernike modes into quantum optics, where they can serve as spatial degrees of freedom for encoding quantum information. Their well-defined aberration structure and rotational symmetries make them physically meaningful and experimentally accessible, rather than purely abstract mathematical constructs.

We work with generalized pupil functions P characterized by a nonuniform amplitude transmission function A and a real phase aberration Φ. We adopt the definition of Zernike disk polynomials using exponential rather than trigonometric azimuthal dependence. Accordingly, the generalized pupil function P is expanded, e.g., in polar coordinates, $\rho = \sqrt{x^2 + y^2}$, $\quad \theta = \arctan(y/x)$, see Fig. 1, as

$$\begin{aligned} P(\rho, \theta) &= A(\rho, \theta) \exp[i\Phi(\rho, \theta)] \\ &= \sum_{n=0}^{\infty} \sum_{m=-n}^{n} a_{mn} Z_n^m(\rho, \theta), \\ & 0 \leqslant \rho \leqslant 1, \quad 0 \leqslant \theta < 2\pi, \end{aligned} \tag{1}$$

in which the normalized polynomials are expressed in terms of radial polynomials $R_n^{|m|}(\rho)$ [10] as

$$Z_n^m(\rho, \theta) = \sqrt{n+1}\, R_n^{|m|}(\rho) e^{im\theta}, \tag{2}$$

$$R_n^{|m|}(\rho, \theta) = \sum_{k=0}^{\frac{n-|m|}{2}} \frac{(-1)^k (n-k)!}{k!\left(\frac{n+m}{2} - k\right)!\left(\frac{n-m}{2} - k\right)!} \rho^{n-2k}, \tag{3}$$

and where n and m in the summation are integers such that $n - |m|$ is even and nonnegative. The coefficients a_{mn} are given by

$$a_{mn} = \frac{1}{\pi} \int \mathrm{d}^2\rho\, P(\boldsymbol{\rho}) Z_n^m(\boldsymbol{\rho}), \tag{4}$$

where $\boldsymbol{\rho} = (\rho, \theta)$, $\mathrm{d}^2\rho = \rho\, \mathrm{d}\rho \mathrm{d}\theta$, and the integration is performed over the pupil region (1). The form (2) provides great simplification in computing diffraction integrals due to the separation of variables [24]. When the system is aberration-free, $A = 1$, $\Phi = 0$ in the pupil. Note that most authors in the optics community consider uniform amplitude transmission pupils $A = 1$ and expand only the aberration phase Φ into Zernike polynomials.

The orthogonality and completeness relations of the polynomials are as follows:

$$\int d^2\rho\, Z_n^{m*}(\boldsymbol{\rho}) Z_{n'}^{m'}(\boldsymbol{\rho}) = \pi\,\delta_{nn'}\delta_{mm'}, \tag{5}$$

$$\sum_{mn} Z_n^{m*}(\boldsymbol{\rho}) Z_n^{m}(\boldsymbol{\rho}') = \pi\,\delta(\boldsymbol{\rho}-\boldsymbol{\rho}'). \tag{6}$$

The number of linearly independent polynomials of degree $\leqslant n$ is $\frac{1}{2}(n+1)(n+2)$ [12]. Hence, every polynomial in (x, y) can be expressed as a linear combination of a finite number of polynomials Z_n^m, which means the set is complete [10]. A product of two polynomials are linearized as [25,26]

$$Z_{n_1}^{m_1}(\boldsymbol{\rho}) Z_{n_2}^{m_2}(\boldsymbol{\rho}) = \sum_{n_3} A_{n_1 n_2 n_3}^{m_1 m_2, m_1+m_2}\, Z_{n_3}^{m_1+m_2}(\boldsymbol{\rho}). \tag{7}$$

Here the summation is over all nonnegative integers n_3 with

$$\text{parity}(n_3) = \text{parity}(m_3) = \text{parity}(m_1+m_2), \tag{8}$$

$m_3 = m_1 + m_2$ such that $\max(|m_3|, |n_1 - n_2|) \leqslant n_3 \leqslant n_1 + n_2$. There are at most $\min\{n_1, n_2\} + 1$ terms in the sum. The A's are given by the Clebsch-Gordan coefficients [27]

$$A_{n_1 n_2 n_3}^{m_1 m_2 m_3} = \sqrt{\frac{n_3+1}{(n_1+1)(n_2+1)}}\left|C_{\frac{m_1}{2}\frac{m_2}{2}\frac{m_3}{2}}^{\frac{n_1}{2}\frac{n_2}{2}\frac{n_3}{2}}\right|^2, \tag{9}$$

which are nonvanishing only when

$$n_1, n_2, n_3 = \text{integers or half-integers} \geqslant 0, \tag{10}$$

such that

$$\frac{n_1}{2} + \frac{n_2}{2} + \frac{n_3}{2} = \text{integer}, \tag{11}$$

while satisfying the triangle conditions

$$|n_r - n_s| \leqslant n_t \leqslant n_r + n_s \tag{12}$$

for any permutation r, s, t of $1, 2, 3$, and when $m_r = -n_r, -n_r + 1, \ldots, n_r - 1, n_r$, $r = 1, 2, 3$, with $m_1 + m_2 - m_3 = 0$.

The Fourier transforms of the Zernike polynomials are computed to be [28]

$$\begin{aligned}\tilde{Z}_n^m(\boldsymbol{q}) &= \int_0^1 d\rho\,\rho \int_0^{2\pi} d\theta\, Z_n^m(\rho,\theta) e^{2\pi i \rho q \cos(\theta-\phi)} \\ &= 2\pi i^n \sqrt{n+1}\frac{J_{n+1}(2\pi q)}{2\pi q} e^{im\phi},\end{aligned} \tag{13}$$

where $\boldsymbol{q} = (q, \phi)$. Note that the index m is associated only with the angular factor $e^{im\phi}$ while the index n—with radial factor $J_{n+1}(2\pi q)/(2\pi q)$. The $\tilde{Z}_n^m$ are orthogonal and complete over the entire space

$$\int_{-\infty}^{\infty} d^2q\, \tilde{Z}_n^{m*}(\boldsymbol{q}) \tilde{Z}_{n'}^{m'}(\boldsymbol{q}) = \pi\,\delta_{mm'}\delta_{nn'}, \tag{14}$$

$$\sum_{mn} \tilde{Z}_n^{m*}(\boldsymbol{q}) \tilde{Z}_n^{m}(\boldsymbol{q}') = \pi\,\delta(\boldsymbol{q}-\boldsymbol{q}'), \tag{15}$$

as can be checked using Eqs. (5) and (6), the orthogonality of sines and cosines as well as Bessel functions

$$\int_0^{\infty} \frac{dt}{t} J_{m+2p+1}(t) J_{m+2q+1}(t) = \frac{\delta_{pq}}{2(m+2p+1)}. \tag{16}$$

III. TRANSFORMATIONS IN ZERNIKE BASIS

To utilize Zernike modes as a resource for quantum information processing, it is essential to establish viable methods for their experimental generation, manipulation, and measurement. In this section, we outline a sequence of practical procedures that enable full control over photon wave packets in the Zernike basis. We begin by describing methods for mode preparation using interferometric and holographic techniques. We then examine how these modes evolve under free-space propagation and optical transformation. Following this, we discuss mode conversion strategies based on the symmetry properties of Zernike modes, and finally, we present detection schemes that project incoming quantum states onto specific Zernike modes for measurement.

A. Preparation

The preparation of photons in specific Zernike modes is a crucial first step toward implementing quantum information protocols based on this basis. Zernike modes, defined on the unit disk, are suited to be encoded in the spatial profile of a light field across a circular aperture. To imprint these profiles onto photons, one can use spatial light modulation techniques that are already standard in classical optics and wavefront control.

One widely used method is the application of computer-generated holographic masks [16,29]. These are diffractive optical elements designed to transform an incoming Gaussian or plane wave into a desired, Zernike, mode in the present case, by modulating its amplitude and phase. Such holograms can be fabricated using spatial light modulators (SLMs), digital micromirror devices [30], and they can be dynamically reprogrammed to generate different modes on demand. Zernike phase patterns can be generated using the same technology as Laguerre-Gaussian (LG) beams, including phase-only SLMs and diffractive optics. Higher-order Zernikes exhibit finer radial structure, requiring sufficient pixel resolution to maintain fidelity.

For commercially available SLMs with pixel pitches of 8–20 µm, diffraction efficiencies of 60 to 85% have been reported for comparable spatial frequencies [31], implying similar overall transmission for single-photon operation.

Another practical technique involves an interferometric generation of Zernike modes using a Twyman-Green interferometer [12]. In this setup, the beam is split into two parts and one arm is modified by inserting a known optical aberration (such as a lens with known aberration, or a deformable mirror). When the two arms are recombined, the resulting interference pattern encodes the desired Zernike phase structure.

For single-photon states, these classical field modulation methods can be directly applied to the spatial profile of a single photon using a transmissive or reflective SLM. The hologram effectively acts as a projection operator, transforming an incoming photon wavefront into a specific Zernike spatial profile. The success of this transformation can be verified by observing the resulting diffraction pattern in the Fourier plane or by mode-selective detection downstream.

Thus, the preparation of Zernike modes leverages existing tools in classical beam shaping and wavefront engineering, making this quantum-optical implementation both conceptually accessible and experimentally feasible.

B. Image space

In Fourier optics, the image of an object is the convolution of the image predicted by geometrical optics with the Fraunhofer diffraction pattern of the exit pupil [32]. Now, the Fourier transforms (13) can be generated as Frounhofer pattern of the Zernike field profile. This can be done in the focal plane of a spherical lens with focal length f:

$$\tilde{Z}_n^m(\boldsymbol{\rho}) = \frac{k}{2\pi f}\int \mathrm{d}\boldsymbol{\rho}'\, Z_n^m(\boldsymbol{\rho}')e^{-i\frac{k}{f}\boldsymbol{\rho}\cdot\boldsymbol{\rho}'} = 2\pi i^n\sqrt{n+1}\,\frac{J_{n+1}(2\pi\rho k/f)}{2\pi\rho}e^{im\phi}. \tag{17}$$

The amplitude and phase of the light at coordinates (ρ_x, ρ_y) in the focal plane are determined by the amplitude and phase of the input Fourier component at spatial frequencies $(q_x = k\rho_x/f, q_y = k\rho_y/f)$. From Eq. (17) it is seen that when a pupil function is expanded in the Zernke basis as in Eq. (1), the spatial spectrum of the pupil function itself may be associated with the amplitude distribution in the image plane

$$\tilde{P}(\boldsymbol{q}) = \sum_{mn} a_{mn}\tilde{Z}_n^m(\boldsymbol{q}), \tag{18}$$

with the same expansion coefficients. This means that a function in the pupil plane expressed as a series of Zernike polynomials $Z_n^m(\boldsymbol{\rho})$ immediately yields its image plane function by the simple substitution of the $\tilde{Z}_n^m(\boldsymbol{q})$ for $Z_n^m(\boldsymbol{\rho})$. It should be noted that the series expansion for the *wavefront* distortion in the pupil does not have this simple representation. This procedure may be used to calculate the diffraction patterns in the image plane of an optical system.

C. Propagation

Applying the Fresnel diffraction operator to the Zernike profile at $z = 0$ one gets

$$Z_n^m(\boldsymbol{\rho}, z) = -\frac{ike^{ikz}}{z\pi}\int \mathrm{d}^2\rho' Z_n^m(\boldsymbol{\rho}')e^{\frac{ik}{2z}|\boldsymbol{\rho}-\boldsymbol{\rho}'|^2} = -\frac{ik}{z}e^{ikz+\frac{ik\rho^2}{2z}}e^{im\theta}V_n^m(\rho; z), \tag{19}$$

where we integrate the theta part and define

$$V_n^m(\rho; z) \equiv i^m\sqrt{n+1}\int_0^1 \mathrm{d}\rho'\rho' R_n^m(\rho') \times J_m\left(-\frac{k\rho\rho'}{z}\right)\exp\left[\frac{ik}{2z}\rho'^2\right]. \tag{20}$$

This integral was evaluated by [26] as a Bessel-Bessel series. The coefficients V_n^m are

$$V_n^m(\rho; z) = \sqrt{n+1}e^{-\frac{ik}{4z}}\sum_h \sum_{l=\frac{|n-h|}{2}}^{\frac{n+h}{2}} i^{l-h}(2l+1) \times A_{2l,n,h}^{0,m,m}\, j_l\left(-\frac{k}{4z}\right)\frac{J_{h+1}(2\pi\rho)}{2\pi\rho}, \tag{21}$$

where j_l is the spherical Bessel function, and the summation is over all h of same parity as m with $h \geqslant |m|$. Due to the decay properties of (spherical) Bessel functions with increasing order, the number of terms to be used in the double series in Eq. (21) should be slightly larger than $\pi\rho k/z$. The summations can be limited to values of h up to a little beyond $\pi e\rho$ and values of l up to a little beyond $ek/(8z)$ [26]. Note also, that for Fraunhofer zone $z \gg k \times$ (pupil area), only the spherical Bessel function for the $l = 0$ (and $h = n$) case $j_0(\beta) = \sin(\beta)/\beta \to 1$ survives the sum for small β, i.e., $V_n^m(\rho; z) \to \sqrt{n+1}\, i^{-n}\frac{J_{n+1}(2\pi\rho)}{2\pi\rho}$ and Eq. (19) becomes proportional to Eq. (17).

D. Mode conversion

Due to the symmetry properties of Zernike modes, the modes with the same n index and $\pm m$ differ from each other by rotation. Hence, these modes can be achieved one from the other by placing a beam rotator in between. The beam rotator is made of two dove prisms, and if one of them rotated about the optical axis by $\theta/2$, then the amplitude distribution of the field will rotate by θ. To change the mode index n, conventional techniques can be used to add or subtract aberrations [22].

A Zernike mode Z_n^m can be modified by adding a controlled aberration profile $\Delta\Phi(\rho, \theta)$ in the pupil plane. If introduce $\Delta\Phi(\rho, \theta) = \alpha Z_{\Delta n}^m(\rho, \theta)$, the product of the original mode and the new profile, according to product rule (7), will be $Z_n^m Z_{\Delta n}^m = \sum_{n'} A_{n,\Delta n,n'}^{mm2m} Z_{n'}^{2m}$. The Clebsch-Gordan structure of A determines which n' values appear, effectively "shifting" the radial index n. In practice, such an aberration can be applied by a spatial light modulator or a deformable mirror programed with the desired $Z_{\Delta n}^m$ pattern. The resulting field after renormalization will have a changed radial index.

E. Detection

To detect a photon in the Zernike basis, the holographic mask of the corresponding mode interferogram should be placed before the conventional detector system in the optical Fourier recognition setup [22,32].

IV. QUANTIZATION IN ZERNIKE MODES

In this section, we proceed with the quantization procedure using Zernike modes. We define the Zernike mode creation operators as

$$z_n^{m\dagger} = \frac{1}{\sqrt{\pi}}\int \mathrm{d}^2q\,\tilde{Z}_n^m(\boldsymbol{q})a^\dagger(\boldsymbol{q}), \tag{22}$$

$$a^\dagger(\boldsymbol{q}) = \frac{1}{\sqrt{\pi}}\sum_{mn}\tilde{Z}_n^{m*}(\boldsymbol{q})z_n^{m\dagger}, \tag{23}$$

obeying the commutation relations

$$\left[\tilde{z}_n^m, \tilde{z}_{n'}^{m'\dagger}\right] = \int \mathrm{d}^2 q\, \tilde{Z}_n^{m*}(\boldsymbol{q})\tilde{Z}_{n'}^{m'}(\boldsymbol{q}) = \delta_{mm'}\delta_{nn'}. \tag{24}$$

Here $a^\dagger(\boldsymbol{q})$ and $a(\boldsymbol{q})$ are the usual bosonic creation and annihilation operators for plane wave modes with transverse wave vector $\boldsymbol{q}$, satisfying the usual commutation relations $[a(\boldsymbol{q}), a^\dagger(\boldsymbol{q}')] = \delta(\boldsymbol{q}-\boldsymbol{q}')$. While the polarization degree of freedom could, in principle, be included in the analysis, it plays no essential role in the discussions that follow. For simplicity, we assume the creation operator is implicitly summed over polarization states, i.e., $a^\dagger(\boldsymbol{q}) = \frac{1}{\sqrt{2}}\sum_s a_s^\dagger(\boldsymbol{q})$. Then, it can be seen that the states defined as

$$\tilde{z}_n^{m\dagger}|0\rangle = \left|\tilde{z}_n^m\right\rangle, \tag{25}$$

are orthonormal and complete

$$\left\langle\tilde{z}_n^m\middle|\tilde{z}_{n'}^{m'}\right\rangle = \delta_{mm'}\delta_{nn'}, \tag{26}$$

$$\sum_{n=0}^{\infty}\sum_{m=-n(2)}^{n}\left|\tilde{z}_n^m\right\rangle\!\left\langle\tilde{z}_n^m\right| = I, \tag{27}$$

where $\sum_{m=-n(2)}^{n}$ indicates that the sum is over m in the range $\{-n, -n+2, \dots, n\}$.

A. Field operator and the first-order correlation function

The angular spectrum representation [10] of the field operator

$$\mathsf{E}^{(+)}(\mathbf{r}) = \int \frac{\mathrm{d}^2 q}{(2\pi)^2}\, a(\boldsymbol{q})e^{i(\boldsymbol{q}\cdot\boldsymbol{\rho}+\sqrt{k^2-q^2}z)}, \tag{28}$$

in paraxial approximation ($\sqrt{k^2-q^2}\to k-\frac{q^2}{2k}$) in terms of the Zernike mode annihilation operators $\tilde{z}_n^m$ has the form

$$\begin{aligned}\mathsf{E}^{(+)}(\mathbf{r}) &= \frac{e^{ikz}}{\sqrt{\pi}}\sum_{mn}\tilde{z}_n^m\int\frac{\mathrm{d}^2 q}{(2\pi)^2}\tilde{Z}_n^m(\boldsymbol{q})e^{i\left(\boldsymbol{q}\cdot\boldsymbol{\rho}-\frac{q^2 z}{2k}\right)}\\ &= \frac{ke^{ikz}}{2iz\pi^{\frac{3}{2}}}\sum_{mn}\tilde{z}_n^m\int \mathrm{d}^2\rho' Z_n^m(\boldsymbol{\rho}')e^{\frac{ik}{2z}|\boldsymbol{\rho}-\boldsymbol{\rho}'|^2}\\ &= \frac{ke^{ikz+\frac{ik\rho^2}{2z}}}{iz\sqrt{\pi}}e^{im\theta}\sum_{mn}V_n^m(\rho;z)\,\tilde{z}_n^m,\end{aligned} \tag{29}$$

where V_n^m are given in Eq. (21). The field operator assumes a particularly simple form in the Fraunhofer region (cf. Sec. III B)

$$\mathsf{E}^{(+)}(\mathbf{r}) = e^{ikz}\sum_{mn}\tilde{Z}_n^m(\rho_x,\rho_y)\,\tilde{z}_n^m, \tag{30}$$

with $\rho_{x(y)} = f q_{x(y)}/k$.

B. Single-photon state in the Zernike basis

Now using the orthonormality of the Fourier transforms of the Zernike polynomials (14), one can expand any state in the Zernike basis using their closure relation. Particularly, a paraxial single-photon state, $|\psi_1\rangle = \int\frac{\mathrm{d}^2 q}{(2\pi)^2}C(\mathbf{k})a^\dagger(\mathbf{k})|0\rangle$, where $C(\mathbf{k})$ is strongly concentrated around $\mathbf{k}_0 = k_0\hat{\mathbf{z}}$ with a small transverse part $|\boldsymbol{q}|\leqslant\vartheta_0 k_0$, can be written as

$$|\psi_1\rangle = \sum_{mn}\left|\tilde{z}_n^m\right\rangle\!\left\langle\tilde{z}_n^m\middle|\psi_1\right\rangle \equiv \sum_{mn}\zeta_n^m\left|\tilde{z}_n^m\right\rangle, \tag{31}$$

where (relabeling $\mathbf{k}$ using $\boldsymbol{q}$)

$$\zeta_n^m = \left\langle z_n^m\middle|\psi_1\right\rangle = \int \mathrm{d}^2 q\, C(\boldsymbol{q})\tilde{Z}_n^{m*}(\boldsymbol{q}). \tag{32}$$

From now on we will work only with paraxial states.

C. First-order correlation function

The first-order correlation function $G^{(1)}(\mathbf{r};\mathbf{r}) \equiv G^{(1)}(\mathbf{r}) = \langle\psi_1|\mathsf{E}^{(-)}(\mathbf{r})\mathsf{E}^{(+)}(\mathbf{r})|\psi_1\rangle$ also assumes a particularly simple form in the Fraunhofer region

$$G^{(1)}(\mathbf{r}) = \sum_{\substack{m_1m_2\\n_1n_2}}\zeta_{n_1}^{m_1}\zeta_{n_2}^{m_2*}\tilde{Z}_{n_1}^{m_1}(\rho_x,\rho_y)\tilde{Z}_{n_2}^{m_2*}(\rho_x,\rho_y). \tag{33}$$

Equation (33) satisfies the first-order coherence condition, as expected for any pure single-photon state. For a pure single-photon state $|\psi_1\rangle$ to satisfy the coherence condition, it is required that the first-order correlation function as defined $G_{ij}^{(1)}(\mathbf{r}_1;\mathbf{r}_2) = \langle\psi_1|\mathsf{E}_i^{(-)}(\mathbf{r}_1)\mathsf{E}_j^{(+)}(\mathbf{r}_2)|\psi_1\rangle$ $(i,j = x,y,z)$, to factorize into a function of $\mathbf{r}_1$, i and a function of $\mathbf{r}_2$, j. [33] [Chap. 12.7.4].

D. Two-photon state in the Zernike basis

The most general paraxial two-photon state

$$|\psi_2\rangle = \frac{1}{\sqrt{2}}\iint \mathrm{d}^2 q_1\mathrm{d}^2 q_2\, C(\boldsymbol{q}_1,\boldsymbol{q}_2)a^\dagger(\boldsymbol{q}_1)a^\dagger(\boldsymbol{q}_2)|0\rangle, \tag{34}$$

$$\langle\psi_2|\psi_2\rangle = 1, \tag{35}$$

can be represented in the two-photon Zernike basis. The latter can be constructed using tensor products of one-photon Zernike basis states as

$$\begin{aligned}\left|z_{n_1}^{m_1}, z_{n_2}^{m_2}\right\rangle = \frac{1}{\pi\sqrt{2}}\iint \mathrm{d}^2 q_1\mathrm{d}^2 q_2\tilde{Z}_{n_1}^{m_1}(\boldsymbol{q}_1)\tilde{Z}_{n_2}^{m_2}(\boldsymbol{q}_2)\\ \times\, a^\dagger(\boldsymbol{q}_1)a^\dagger(\boldsymbol{q}_2)|0\rangle.\end{aligned} \tag{36}$$

Expanding the above two-photon state in the tensor product Zernike basis, we get

$$|\psi_2\rangle = \sum_{\substack{m_1m_2\\n_1n_2}}\zeta_{n_1n_2}^{m_1m_2}\left|z_{n_1}^{m_1}, z_{n_2}^{m_2}\right\rangle, \tag{37}$$

with

$$\begin{aligned}\zeta_{n_1n_2}^{m_1m_2} &\equiv \left\langle z_{n_1}^{m_1}, z_{n_2}^{m_2}\middle|\psi_2\right\rangle\\ &= \frac{1}{\pi}\iint \mathrm{d}^2 q_1\,\mathrm{d}^2 q_2\, C(\boldsymbol{q}_1,\boldsymbol{q}_2)\tilde{Z}_{n_1}^{m_1*}(\boldsymbol{q}_1)\tilde{Z}_{n_2}^{m_2*}(\boldsymbol{q}_2).\end{aligned} \tag{38}$$

The normalization condition (35) is equivalent to

$$\sum_{\substack{m_1m_2\\n_1n_2}}\left|\zeta_{n_1n_2}^{m_1m_2}\right|^2 = 1. \tag{39}$$

E. Second-order correlation function

With the help of Eqs. (30) and (37) the second-order correlation function in the Zernike basis assumes the form

$$G^{(2)}(\mathbf{r}_1,\mathbf{r}_2) = 4 \sum_{\substack{m_1m_2m_3m_4\\ n_1n_2n_3n_4}} \zeta_{n_1n_2}^{m_1m_2}\zeta_{n_3n_4}^{m_3m_4*} \times \tilde{Z}_{n_1}^{m_1}(\rho_{x_1},\rho_{y_1})\,\tilde{Z}_{n_2}^{m_2}(\rho_{x_2},\rho_{y_2}) \times \tilde{Z}_{n_3}^{m_3*}(\rho_{x_1},\rho_{y_1})\,\tilde{Z}_{n_4}^{m_4*}(\rho_{x_2},\rho_{y_2}). \tag{40}$$

F. Two-photon state from the down-conversion process

Equation (38) holds for the specific symmetric amplitude such as the one generated from the process of SPDC [34]

$$C(\boldsymbol{q}_1,\boldsymbol{q}_2) = \sqrt{\frac{2L}{\pi^2K}}v(\boldsymbol{q}_1+\boldsymbol{q}_2)\mathrm{sinc}\left(\frac{L(|\boldsymbol{q}_1-\boldsymbol{q}_2|^2)}{4K}\right) \propto v(\boldsymbol{q}_1+\boldsymbol{q}_2), \quad \text{in thin crystal approx.} \tag{41}$$

Here $v(\boldsymbol{q}_p)$ is the angular spectrum of the pump beam with $\boldsymbol{q}_p = \boldsymbol{q}_1 + \boldsymbol{q}_2$, L is the length of the nonlinear crystal in the propagation (z) direction, and K is the magnitude of the pump field wave vector. The thin-crystal approximation is a well-established simplification in SPDC theory to simplify the phase-matching function when the nonlinear crystal length L is small compared to the Rayleigh range of the pump beam. In this limit, the sinc phase-matching function becomes broad in momentum space, and the two-photon amplitude is effectively determined by the spatial profile of the pump [20,34].

Now, making the following change of variables

$$\boldsymbol{q}_p = \boldsymbol{q}_1 + \boldsymbol{q}_2, \quad \mathbf{Q} = \tfrac{1}{2}(\boldsymbol{q}_1 - \boldsymbol{q}_2), \tag{42}$$

Eq. (38), in the thin crystal approximation [34], takes the form

$$\zeta_{n_1n_2}^{m_1m_2} = \frac{1}{\pi}\int d^2\rho\, V(\boldsymbol{\rho}) Z_{n_1}^{m_1*}(\boldsymbol{\rho}) Z_{n_2}^{m_2*}(\boldsymbol{\rho}), \tag{43}$$

where $V(\boldsymbol{\rho})$ is the pump profile (the inverse Fourier transform of the angular spectrum of the pump). In the above representation, we make use of the convolution theorem, and change the order of integration. Expanding the pump profile in the Zernike basis $V(\boldsymbol{\rho}) = \sum_{mn} a_{mn} Z_n^m(\boldsymbol{\rho})$, Eq. (43) takes the form

$$\zeta_{n_1n_2}^{m_1m_2} = \sum_{mn} a_{mn} A_{n_1n_2n}^{m_1m_2m}, \tag{44}$$

where we use the orthogonality of Zernike polynomials and the relation (7) [26]. The property $m = m_1 + m_2$ of the Clebsch-Gordan coefficients guarantees that the azimuthal frequency of the initial aberration is conserved in the down-conversion process. In principle, this conservation could be satisfied by fields that exhibit a classical or quantum correlation (entanglement) of aberrations. The other conditions (8) to (12) on the Clebsch-Gordan coefficients lead to additional conservation criteria. These rules mean that in SPDC with a pump in mode Z_n^m, not only m is conserved through $m = m_1 + m_2$, but also only those (n_1, n_2) combinations satisfying the above constraints will appear in the two-photon state. We note here that the conditions are not restrictions on individual indices of signal and idler photons but involve sums and differences. Thus, there is, indeed, a correlation between the indices of the signal and the idler fields. In the next subsection, we show that these conservation conditions lead to aberration entanglement of the down-converted photons.

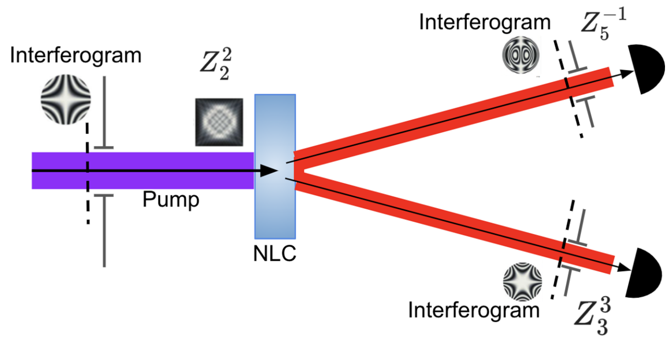

FIG. 2. Schematic of two-photon Zernike mode entanglement via SPDC. A pump beam prepared in a Zernike mode Z_n^m illuminates a thin nonlinear crystal, producing signal and idler photons whose spatial modes are correlated. The dashed lines in front of the pupils represent the interferograms pictured near them. The picture near the nonlinear crystal (NLC) represents the propagated pump profile according to Eq. (17). The conservation of azimuthal quantum number ($m = m_1 + m_2$) and triangle conditions for $n-$indices, arising from Clebsch-Gordan coefficients, govern the resulting two-photon entangled state in the Zernike basis.

G. Entanglement in Zernike modes

We consider the pump profile having a single Zernike mode Z_n^m, so that the expansion coefficients (44) are given only by $a_{mn}A_{n_1n_2n}^{m_1m_2m}$. (See Fig. 2 for a schematic depiction of the two-photon Zernike entanglement setup.)

To verify that the two-photon state is entangled in the Zernike basis, we examine the reduced density matrix of one photon and test its purity via the trace of its square, $\mathrm{Tr}\rho_1^2$. For any pure bipartite state, $\mathrm{Tr}\rho_1^2 = 1$ if and only if the state is separable; $\mathrm{Tr}\rho_1^2 < 1$ indicates entanglement. Now, the reduced density matrix for, say, the signal photon of the two-photon state (37) is given by

$$\rho_1 = \sum_{n_1m_1}\sum_{n_1'm_1'} \Xi_{n_1n_1'}^{m_1m_1'} \left|z_{n_1}^{m_1}\right\rangle\!\left\langle z_{n_1'}^{m_1'}\right|, \tag{45}$$

where $\Xi_{n_1n_1'}^{m_1m_1'} \equiv \sum_{n_2m_2} \zeta_{n_1n_2}^{m_1m_2}\zeta_{n_1'n_2}^{m_1'm_2*}$. Note that

$$\Xi_{n_1n_1'}^{m_1m_1'} = \Xi_{n_1'n_1}^{m_1'm_1*}. \tag{46}$$

If the above density matrix represents a mixed state then $|\psi_2\rangle$ is entangled. From the properties of density matrices $\mathrm{Tr}\rho_1 = 1$ and $\rho_1 \geqslant 0$ it follows that

$$\sum_{n_1m_1} \Xi_{n_1n_1}^{m_1m_1} = 1, \quad \Xi_{n_1n_1}^{m_1m_1} \geqslant 0. \tag{47}$$

The condition $\mathrm{Tr}\rho_1^2 \leqslant 1$ follows from the fact that ρ_1 is a normalized positive semidefinite operator. Here $\rho_1 > 0$ means that all eigenvalues of ρ_1 are nonnegative. The condition $\mathrm{Tr}\rho_1^2 \leqslant 1$ is equivalent to $\sum_{\substack{n_1m_1\\ n_1'm_1'}} |\Xi_{n_1n_1'}^{m_1m_1'}|^2 \leqslant 1$, where we use the orthogonality of the Zernike modes and the symmetry property (46). Subtracting $\sum_{n_1m_1} \Xi_{n_1n_1}^{m_1m_1} \sum_{n_1'm_1'} \Xi_{n_1'n_1'}^{m_1'm_1'} = 1$

[cf. Eq. (47)] from each side of the last inequality, we have

$$\sum_{\substack{n_1 m_1\\ n_1' m_1'}} \left[\left| \Xi^{m_1 m_1'}_{n_1 n_1'} \right|^2 - \Xi^{m_1 m_1}_{n_1 n_1} \Xi^{m_1' m_1'}_{n_1' n_1'} \right] \leqslant 0. \tag{48}$$

Since ρ_1 is a positive-semidefinite operator, its elements $\Xi^{m_1 m_1'}_{n_1 n_1'} = \langle z^{m_1}_{n_1} | \rho_1 | z^{m_1'}_{n_1'} \rangle$ obey the generalized Cauchy-Schwartz-Buniakowski inequality

$$\left| \Xi^{m_1 m_1'}_{n_1 n_1'} \right|^2 \leqslant \Xi^{m_1 m_1}_{n_1 n_1} \Xi^{m_1' m_1'}_{n_1' n_1'}, \tag{49}$$

for any n_1, m_1, n_1', m_1', which means that all the terms in the summation in Eq. (48) are either zero or negative. Then, if at least one $|\Xi^{m_1 m_1'}_{n_1 n_1'}|^2 - \Xi^{m_1 m_1}_{n_1 n_1} \Xi^{m_1' m_1'}_{n_1' n_1'}$ is nonzero, the *equality* in Eq. (48) cannot hold, indicating that ρ_1 is a mixed state ($\mathrm{Tr}[\rho_1^2] < 1$) and, consequently, $|\psi_2\rangle$ must be entangled. Note that for $|\Xi^{m_1 m_1'}_{n_1 n_1'}|^2 - \Xi^{m_1 m_1}_{n_1 n_1} \Xi^{m_1' m_1'}_{n_1' n_1'} < 0$ it must be that $\Xi^{m_1 m_1}_{n_1 n_1} > 0$ and $\Xi^{m_1' m_1'}_{n_1' n_1'} > 0$. With the help of Eq. (8) we see that

$$\mathrm{parity}(m_1 + m_2) = \mathrm{parity}(m), \tag{50}$$

$$\mathrm{parity}(m_1' + m_2) = \mathrm{parity}(m), \tag{51}$$

hence it must be that

$$\mathrm{parity}(m_1) = \mathrm{parity}(m_1'), \tag{52}$$

otherwise $\Xi^{m_1 m_1'}_{n_1 n_1'} = 0$. Thus, even if $\mathrm{parity}(m_1) \neq \mathrm{parity}(m_1')$, there still can be terms with $\Xi^{m_1 m_1}_{n_1 n_1} \neq 0$ and $\Xi^{m_1' m_1'}_{n_1 n_1} \neq 0$ but $\Xi^{m_1 m_1'}_{n_1 n_1'} = 0$. Noting also the second condition (47), we conclude that $|\psi_2\rangle$ is entangled in the Zernike modes.

V. DISCUSSION

The presence of entanglement in the Zernike basis is not merely a formal consequence of the mathematical framework, it offers practical utility for quantum optics and quantum information science. Like Laguerre-Gaussian or Hermite-Gaussian modes, which are the eigenmodes of free-space propagation, Zernike modes directly correspond to optical aberrations and are the natural eigenmodes of wavefront distortions. This makes them particularly appealing for quantum tasks involving real optical systems, where aberrations naturally occur and must be measured, corrected, or exploited.

In diffraction-limited free-space propagation, the mapping in Eq. (18) ensures that a field decomposed into Zernike modes at the pupil retains the same expansion coefficients in the image plane, avoiding intermode coupling. This property holds for any aperture-limited optical system free of random aberrations, and is a key advantage for encoding and decoding in reimaged pupil planes.

One key application is quantum aberration sensing. In this protocol, a pair of photons entangled in Zernike modes is generated via SPDC. One photon (the probe) is transmitted through an unknown or distorted optical element, while the other (the reference) is routed directly to a detection system. By performing joint measurements in the Zernike basis, one can extract information about the aberration-induced mode transformation of the probe photon. Since Zernike modes diagonalize common aberration types (e.g., defocus, astigmatism, coma), the structure of the entangled state enables efficient inference of aberrations with reduced measurement complexity compared to more generic mode decompositions.

Another promising direction is in high-dimensional quantum communication over aberrated channels. In many realistic scenarios, including propagation through the atmosphere, tissue, or imperfect lenses, channel distortions can be compactly described in terms of Zernike polynomials. In this setting, precompensation or postcorrection of Zernike-mode entangled photons could enable more stable transmission of qudits or entangled states through realistic, imperfect optical media.

Adaptive-optics compensation in a Zernike basis is well established in classical optics. While its application to quantum channels under turbulence is beyond the present scope, it is a natural extension of our framework and will be addressed in a forthcoming study on propagation through random media.

VI. CONCLUSION

We developed a complete theoretical framework for using Zernike modes as a structured, physically grounded basis for quantum information processing. Leveraging the orthogonality, rotational symmetry, and completeness of Zernike polynomials on the unit disk, we constructed single- and two-photon wave packets and showed how these modes evolve under free-space propagation and optical transformations. We demonstrated that two-photon states generated via SPDC are entangled in the Zernike basis, with correlations arising from angular momentum conservation and Clebsch-Gordan selection rules. The results suggest that Zernike modes can serve as a new degree of freedom for quantum information tasks, particularly in systems affected by optical aberrations. We hope that this work encourages further experimental exploration of Zernike-mode-based quantum optics and motivates new applications at the intersection of spatial mode control and quantum technologies.

ACKNOWLEDGMENTS

The authors thank A. Allahverdyan, V. Mkrtchian, and V. Abgaryan for discussions. This work was supported by HESC (Higher Education and Science Committee) of Armenia, Grant No. 24FP-1F030.

DATA AVAILABILITY

No data were created or analyzed in this study.

[1] L. Allen, M. W. Beijersbergen, R. J. C. Spreeuw, and J. P. Woerdman, Phys. Rev. A **45**, 8185 (1992).

[2] V. Y. Bazhenov, M. S. Soskin, and M. V. Vasnetsov, J. Mod. Opt. **39**, 985 (1992).

[3] M. W. Beijersbergen, L. Allen, H. E. L. O. van der Veen, and J. P. Woerdman, Opt. Commun. **96**, 123 (1993).
[4] M. J. Padgett and J. Courtial, Opt. Lett. **24**, 430 (1999).
[5] G. S. Agarwal, J. Opt. Soc. Am. A **16**, 2914 (1999).
[6] A. Mair, A. Vaziri, G. Weihs, and A. Zeilinger, Nature (London) **412**, 313 (2001).
[7] A. Vaziri, G. Weihs, and A. Zeilinger, Phys. Rev. Lett. **89**, 240401 (2002).
[8] F. Zernike, Physica **1**, 689 (1934).
[9] B. R. A. Nijboer, Ph.D. thesis, University of Groningen, The Netherlands, 1942.
[10] M. Born and E. Wolf, *Principles of Optics* (Cambridge University Press, Cambridge, England, 2019).
[11] A. Bhatia and E. Wolf, Proc. Cambridge Philos. Soc. **50**, 40 (1954).
[12] V. N. Mahajan, *Optical Imaging and Aberrations. Part III–Wavefront Analysis* (SPIE, Bellingham, WA, 2013).
[13] F. Zernike and H. C. Brinkman, Proc. Akad. Wet. Amsterdam **38**, 161 (1935).
[14] V. Abgaryan, A. Nersessian, and V. Yeghikyan, arXiv:2504.15713.
[15] G. S. Pogosyan, C. Salto-Alegre, K. B. Wolf, and A. Yakhno, J. Math. Phys. **58**, 072101 (2017).
[16] N. R. Heckenberg, R. McDuff, C. P. Smith, H. Rubinsztein-Dunlop, and M. J. Wegener, Opt. Quant. Electron. **24**, S951 (1992).
[17] A. T. O'Neil and J. Courtial, Opt. Commun. **181**, 35 (2000).
[18] X. Xue, H. Wei, and A. G. Kirk, Opt. Lett. **26**, 1746 (2001).
[19] H. Sasada and M. Okamoto, Phys. Rev. A **68**, 012323 (2003).
[20] S. P. Walborn, A. N. de Oliveira, R. S. Thebaldi, and C. H. Monken, Phys. Rev. A **69**, 023811 (2004).
[21] S. P. Walborn, S. Pádua, and C. H. Monken, Phys. Rev. A **71**, 053812 (2005).
[22] D. Malacara, *Optical Shop Testing* (Wiley & Sons, New York, 2007).
[23] G.-m. Dai, *Wavefront Optics for Vision Correction* (SPIE, Bellingham, WA, 2008).
[24] E. C. Kintner, Opt. Commun. **18**, 235 (1976).
[25] W. J. Tango, Applied Physics **13**, 327 (1977).
[26] S. van Haver and A. J. E. M. Janssen, J. Eur. Opt. Soc.-Rapid Publ. **8**, 13044 (2013).
[27] D. A. Varshalovich, A. N. Moskalev, and V. K. Khersonskii, *Quantum Theory of Angular Momentum* (World Scientific, Singapore, 1988).
[28] R. J. Noll, J. Opt. Soc. Am. **66**, 207 (1976).
[29] S. Fukushima, T. Kurokawa, and M. Ohno, Appl. Phys. Lett. **58**, 787 (1991).
[30] S. A. Goorden, J. Bertolotti, and A. P. Mosk, Opt. Express **22**, 17999 (2014).
[31] M. Mirhosseini, O. S. Magana-Loaiza, C. Chen, B. Rodenburg, M. Malik, and R. W. Boyd, Opt. Express **21**, 30196 (2013).
[32] J. W. Goodman, *Introduction to Fourier Optics* (McGraw-Hill, San Francisco, 1968).
[33] L. Mandel and E. Wolf, *Optical Coherence and Quantum Optics* (Cambridge University Press, Cambridge, 2008).
[34] C. H. Monken, P. H. Ribeiro, and S. Pádua, Phys. Rev. A **57**, 3123 (1998).